

Slow earthquakes triggered by typhoons

ChiChing Liu¹, Alan T. Linde² & I. Selwyn Sacks²

The first reports^{1,2} on a slow earthquake were for an event in the Izu peninsula, Japan, on an intraplate, seismically active fault. Since then, many slow earthquakes have been detected^{3–8}. It has been suggested⁹ that the slow events may trigger ordinary earthquakes (in a context supported by numerical modelling¹⁰), but their broader significance in terms of earthquake occurrence remains unclear. Triggering of earthquakes has received much attention: strain diffusion from large regional earthquakes has been shown to influence large earthquake activity^{11,12}, and earthquakes may be triggered during the passage of teleseismic waves¹³, a phenomenon now recognized as being common^{14–17}. Here we show that, in eastern Taiwan, slow earthquakes can be triggered by typhoons. We model the largest of these earthquakes as repeated episodes of slow slip on a reverse fault just under land and dipping to the west; the characteristics of all events are sufficiently similar that they can be modelled with minor variations of the model parameters. Lower pressure results in a very small unclamping of the fault that must be close to the failure condition for the typhoon to act as a trigger. This area experiences very high compressional deformation but has a paucity of large earthquakes; repeating slow events may be segmenting the stressed area and thus inhibiting large earthquakes, which require a long, continuous seismic rupture.

Taiwan is located along the boundary between the Philippine Sea plate and the Eurasian plate, one of the most active plate boundaries in the world (Fig. 1). The oblique collision between these two plates drives the mountain building¹⁸ and high seismic activity¹⁹ in this area. Taiwan can be divided into three major geologic provinces: the Central Range, the Western Foothills and the Coastal Range²⁰. The Central Range forms the backbone ridge of the island, where the older continental shelf and slope sediments are raised to a maximum elevation of almost 4,000 m by the on-going orogenic process. The Western Foothills, composed of Oligocene to Pleistocene clastic sediments in a fold-and-thrust belt, suffered a destructive earthquake, of moment magnitude $M_w = 7.7$, on 21 September 1999. The third province is the Coastal Range in eastern Taiwan. Neogene rocks in this province were folded into a series of north-northeast-trending anticlines and synclines and have been cut by thrust faults mostly younger than the early Pleistocene epoch²¹.

The uplift rates along the coast, derived both from geodetic levelling for the past two decades²² and from marine terraces for the past 15,000 years²³, show a consistent pattern with uplift of ~ 10 – 20 mm yr⁻¹ at the southern end, decreasing to ~ 0 mm yr⁻¹ at the northern end. Along the central section of the western boundary of this province, a creeping zone about 20 km in length (Fig. 1), monitored with levelling²⁴ and creepmeters²⁵, showed uplift and thrust shortening rates both of 20 mm yr⁻¹. The creep data are characterized by numerous episodic creep events. In the past 100 years, the Coastal Range has had only two earthquakes with local magnitudes $M_L \geq 7$ (Fig. 1) ($M_L = 7.0$ in 1937 and $M_L = 7.3$ in 1951, with surface rupture displacement of ~ 2 m) and 13 $M_L = 6.0$ – 6.7 events;

earthquakes release only a small fraction of the deformation, which accumulates at the rate of 8.2 cm yr⁻¹.

A small network (~ 10 -km aperture) of three borehole strainmeters (dilatometers) of the Sacks–Evertson design²⁶ was installed at the northern end of the creeping zone (Fig. 1, upper inset), beginning in 2002, as part of an integrated geodetic network. They were installed at depths of 200–266 m. Data from all sites exhibit characteristics of good-quality borehole strain data with response to seismic waves, clear solid-earth tidal signals and exponentially slowing contractional strain rates as the site recovers from the hole-drilling disturbance.

Taiwan experiences typhoons frequently, mainly during the second half of the calendar year. The associated lowering of air pressure normally results in a corresponding episode of expansion (positive strain) in the strainmeter data, with the amplitude of the excursion being proportional to the pressure decrease and also dependent on the bulk modulus of the surrounding rock (Fig. 2, inset). Unexpectedly, however, we also observe slow negative strain changes (contraction) coinciding with some typhoons; the largest such event

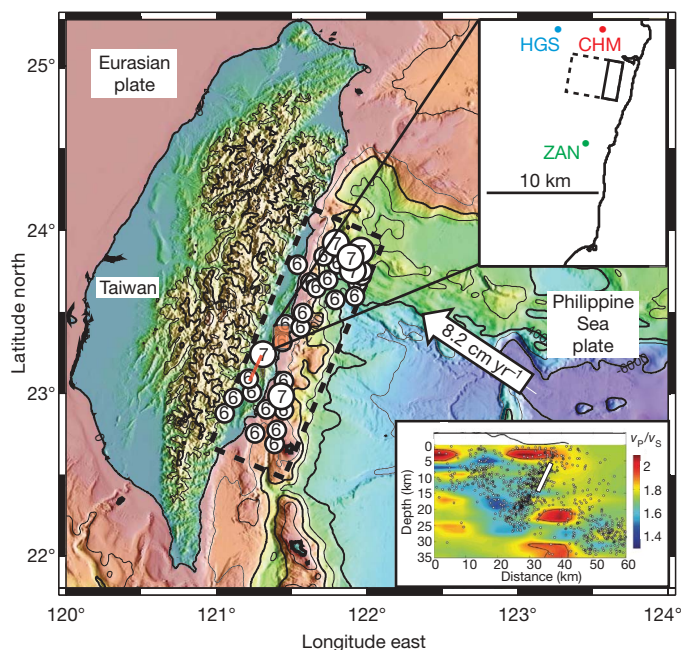


Figure 1 | Topographic map of Taiwan showing collision with Philippine Sea plate. Earthquakes shown (in dashed rectangular area) are all since 1900 and have $M_L > 6$. Of these only one (in 1972) could possibly relieve slip on our model source. Red thick line indicates a creeping zone. Upper inset: study area, showing site locations and plan view of model rupture surface for slow earthquake. Lower inset: seismic section for a profile close to the sites, indicative of a west-dipping normal fault. White rectangle shows location of model rupture. v_p , P-wave velocity; v_s , S-wave velocity.

¹Institute for Earth Sciences, Academia Sinica, 128 Sinica Road, Sec. 2, Nankang, Taipei 115, Taiwan. ²Department of Terrestrial Magnetism, Carnegie Institution of Washington, 5241 Broad Branch Road, NW, Washington DC 20015, USA.

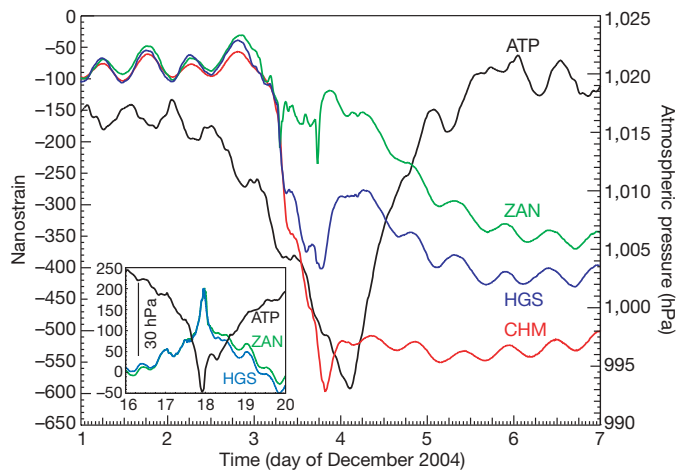


Figure 2 | Strain data for the largest slow event recorded, together with pressure record showing passage of typhoon. Coherent tidal signals are clearly visible. ZAN and HGS, with lower-modulus rock, show greater sensitivity to pressure changes than does CHM, as can be seen in strain rates from 4 to 6 December after the slow earthquake; removal of the pressure effect (Fig. 3) eliminates those trends. All sites experience negative strain changes with some subsequent recovery. This contrasts with the expected behaviour (inset, where the horizontal shows time as day of July 2005), namely that the strain should show expansion followed by recovery due to change of pressure on the surface.

is shown in Fig. 2. From a survey of the strain data (from late 2002 to late 2007), we have identified approximately 20 such strain excursions, all with net contraction (negative strain). These events have durations ranging from hours to more than a day and are detected at all sites recording data at the time of the event. Eleven events, and all those with larger amplitudes and more complex waveform character, occur during the passage of a typhoon. We do not detect any slow events during the typhoon-free first four months of the year. The

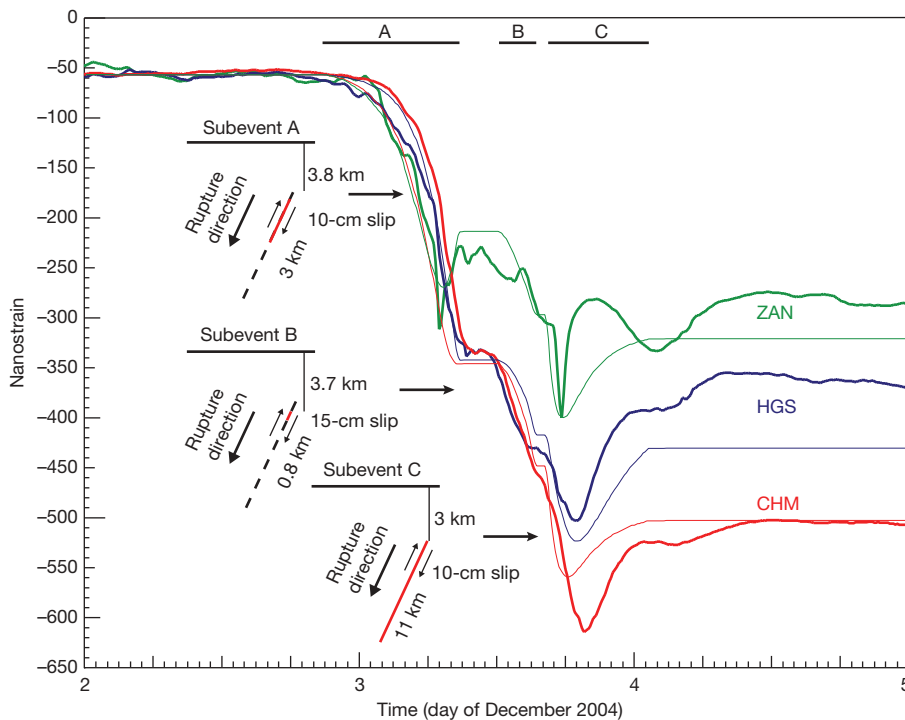


Figure 3 | Data for the same event as in Fig. 2 but after removal of tidal frequencies and atmospheric pressure-induced changes. We divide the event into three stages, indicated by bars A, B and C. Model vertical sections are shown on the left; see Fig. 1 for fault location. Fault lengths are all 3 km.

probability that 11 of these slow strain events coincide with typhoons (28 during our data coverage) by chance is vanishingly small ($<10^{-6}$). (See Supplementary Information for details of this and for additional examples of slow earthquake recordings.)

If these changes were due to surface phenomena associated with the typhoons, we would expect to see them in association with all typhoons; however, most generate only the expected expansion due to lowering of surface pressure (Fig. 2, inset). About half of the events are not associated with typhoon activity. Rather, the slow events must be due to a subsurface source and, given the tectonic setting, the most likely candidate is fault slip with rise time and propagation velocity much less than those for ordinary earthquakes—that is, a slow earthquake.

Original data for the largest observed slow event are shown in Fig. 2; in Fig. 3 we show data for the same event after removing tidal frequencies and strain changes due to atmospheric pressure changes. Sites HGS and ZAN are more influenced by pressure changes than is CHM; that is expected because of the much lower values for bulk modulus at those two sites. Other slow events are similar in character but have smaller amplitudes and are often shorter in duration (corresponding to just the first subevent; see below). The three records have much in common but also have characteristic differences. All sites have initial contraction but ZAN shows a reversal early in the record; all show reversal at a later time. Both the reversals and their differing times are indicative of a propagating source such that a nodal line in the surface strain pattern propagates past the stations and does so at different times.

Three sites do not allow an independent determination of source parameters, so we use local seismicity²⁷ (Fig. 1, lower inset) as a guide for possible source faults. These data indicate, close to our strain-meter net, a subsurface reverse fault dipping to the west with its projected intersection with the surface close to the coastline. In other cross-sections, the data indicate an east-dipping reverse fault farther to the west; we do not show it here, but slip on such a fault can satisfy the data equally well. We assume the west-dipping fault to be a source because this geometry is ideal for increasing the Coulomb criterion

Reverse slip propagates down dip to different depths for the three stages; deeper slip results in a nodal line sweeping past the sites at different times, producing the reversals in strain. All slips are constant along strike and down dip. This provides a good fit to the data.

for failure as a result of lower atmospheric pressure. Typhoons lower pressure on the land but not on the ocean bottom because pressure decrease on the ocean surface is accompanied by a change in sea level such that pressure at depth remains constant; tide-gauge data confirm the increase in sea level. Thus, lower pressure on land both lowers the normal force across the fault and increases the shear stress on a reverse fault, resulting in a slight increase in the likelihood of rupture.

We identify three episodes of slip in this event (Fig. 3) and model accordingly, looking for solutions with sources on the fault indicated by the seismicity. All changes are very slow, so we use static solutions for deformation due to a buried shear dislocation²⁸ and generate a time series by successive calculations for a model with slow propagation of the rupture⁴. Our model (Fig. 3) is comprised of three subevents all starting at about 3-km depth and propagating to different depths; each event has uniform slip along strike and down dip. All sources extend 3 km in the strike direction (N 190° E) and dip 65° W. We use a horizontal line source with slow propagation down dip. For each of these subevents, all sites initially undergo contraction (negative strain) and the sites surround a surface area of positive strain. As the depth of the line source increases, this positive strain area expands, with ZAN being the first site to experience the sign change. Figure 3 shows both the data and the strain time series that result from the model.

This very simple model gives a remarkably good fit to the data. Importantly, we can find a reasonable and simple model for a slow earthquake that satisfies the data. Episodic slip on an east-dipping fault will satisfy the data equally well; both models lead to the same conclusions. The seismic moment release corresponds to an earthquake with magnitude $M_w \approx 5.4$. This event is the largest and most complex we have observed. Some smaller events are similar but most have a much simpler character with waveform similar to the first subevent in the example analysed. Thus, all event data are consistent with a similar source model. The model for the largest event results in surface displacements that are just below the resolution of continuous Global Positioning System sites in the area, consistent with observation.

We plot the magnitudes of the observed strain events versus the pressure changes of the typhoons in Fig. 4. Our modelling assumes an elastic medium, so the strain amplitudes are proportional to the size

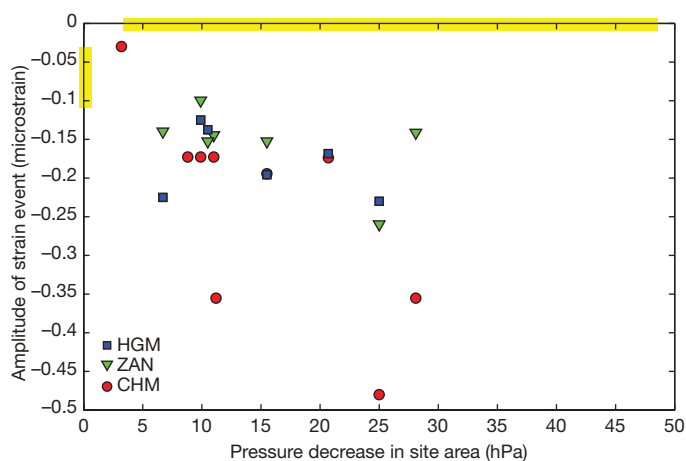


Figure 4 | Amplitudes of the strain signals as a function of pressure drop in the site area as a result of typhoons. The yellow bar along the pressure axis indicates the range of typhoon pressure changes for which no triggered events have been detected; that on the strain axis indicates the size of slow events that occur without typhoon triggering. Scatter in the data set (raw data) prohibit determination of whether event amplitude increases with pressure drop. The CHM data show the largest apparent increase in amplitude; to the extent that that is valid, it is an indication of some variability in the source parameters.

of the slow slip events. On the pressure axis we show, with a yellow bar, the range of pressure drops in the site area for typhoons that do not trigger a slow earthquake; we note that the most severe typhoon did not cause triggering. On the strain axis we show, also with a yellow bar, the range of amplitudes for slow events that occur in the absence of typhoons; all of these are relatively small in comparison with triggered events. There is considerable scatter in the data, with only one site (CHM) apparently showing an increase of strain amplitude with pressure drop. Although more data are necessary before we can investigate this with confidence, it appears that there is some variation of source parameters with the magnitude of the triggering signal.

It has been suggested before that an annual modulation of seismic activity²⁹ (for magnitudes at or below the completeness threshold) is due to the annual change in atmospheric pressure; here we make a definitive connection between fault slip and changes in atmospheric pressure.

We can make a rough estimate of the stress change across the fault interface by assuming an elastic medium. A pressure drop of Δp reduces the vertical stress but the horizontal stress (due to plate convergence) is essentially unaltered because the pressure drop occurs over a large area. This promotes failure both by unclamping ($\Delta p \cos(\theta_{\text{dip}}) \approx 0.8 \text{ kPa}$, reduction in normal force; θ_{dip} , dip angle) and by increasing the reverse shear stress ($\Delta p \sin(\theta_{\text{dip}}) \approx 2 \text{ kPa}$). Stress changes at depth due to seismic waves that cause triggering may be greater by about an order of magnitude¹⁶, so our estimate of the low triggering stress requires that the fault be very close to the failure state; that we do not observe remote seismic triggering suggests that, for a slow earthquake, the trigger duration needs to be longer than that for an ordinary earthquake. At least at the depth of the strainmeters ($\sim 200 \text{ m}$), the strain induced by pressure change is much larger than that of the tides. Our requirement that the fault be critical for triggering is consistent with only a minority of typhoons acting as triggers and slow earthquakes occasionally occurring without a typhoon trigger.

For the slow events not triggered by typhoons, we look for signs of increased levels in background seismic noise as observed in Cascadia⁷ and southwest Japan⁸; typhoon-generated noise precludes any such recognition for the triggered events. We find no such increase in noise level, so these slow events are unaccompanied by a series of long-period earthquakes³⁰.

The total amount of slip (on the fault section common to the subevents) accounts for about four years of plate convergence. The remaining slow events (all much smaller in amplitude), assuming exactly the same source area, require about one to two years of convergence. Although our time window of five years is much too short to enable a meaningful quantitative estimate, it appears that these slow events may be releasing most of the plate convergence on this fault segment.

Our observational program is currently being expanded to have another two small groups of borehole strainmeters, about 90 km to the north and 45 km to the south of the sites involved in this study. From the more northerly area, we have data indicative of another slow earthquake source in that area. The slow events discussed here act to relieve the effects of tectonic compression locally. If there were a number of such sources distributed along this part of the collision zone, they would segment the stressed section such that seismic slip over an extended fault becomes less likely. This may explain why, relative to the high convergence rate (8.2 cm yr^{-1}), there is a paucity of large earthquakes in this area.

Received 8 December 2008; accepted 1 April 2009.
Corrected 15 June 2009.

1. Sacks, I. S., Suyehiro, S., Linde, A. T. & Snoko, J. A. Slow earthquakes and stress redistribution. *Nature* **275**, 599–602 (1978).
2. Sacks, I. S., Suyehiro, S., Linde, A. T. & Snoko, J. A. Stress redistribution and slow earthquakes. *Tectonophysics* **81**, 311–318 (1982).

3. Gladwin, M. T., Gwyther, R. L., Hart, R. H. G. & Brechenridge, K. S. Measurements of the strain field associated with episodic creep events on the San Andreas fault at San Juan Bautista, California. *J. Geophys. Res.* **99**, 4559–4564 (1994).
4. Linde, A. T., Gladwin, M. T., Johnston, M. J. S., Gwyther, R. L. & Bilham, R. G. A slow earthquake sequence on the San Andreas fault. *Nature* **383**, 65–68 (1996).
5. Heki, K., Miyazaki, S. & Tsuji, H. Silent fault slip following an interplate thrust earthquake at the Japan Trench. *Nature* **386**, 595–598 (1997).
6. Crescentini, L., Amoruso, A. & Scarpa, R. Constraints on slow earthquake dynamics from a swarm in central Italy. *Science* **286**, 2132–2134 (1999).
7. Dragert, H., Wang, K. & Rogers, G. Geodetic and seismic signatures of episodic tremor and slip in the northern Cascadia subduction zone. *Earth Planets Space* **56**, 1143–1150 (2004).
8. Ito, Y., Obara, K., Shiomi, K., Sekine, S. & Hirose, H. Slow earthquakes coincident with episodic tremors and slow slip events. *Science* **26**, 503–506 (2006).
9. Linde, A. T. & Sacks, I. S. Slow earthquakes and great earthquakes along the Nankai trough. *Earth Planet. Sci. Lett.* **203**, 265–275 (2002).
10. Kato, N. A possible model for large preseismic slip on a deeper extension of a seismic rupture plane. *Earth Planet. Sci. Lett.* **216**, 17–25 (2003).
11. Rydelek, P. A. & Sacks, I. S. Asthenospheric viscosity inferred from correlated land–sea earthquakes in north-east Japan. *Nature* **336**, 234–237 (1988).
12. Pollitz, F. F. & Sacks, I. S. Consequences of stress changes following the 1891 Nobi earthquake, Japan. *Bull. Seismol. Soc. Am.* **85**, 796–807 (1995).
13. Hill, D. P. *et al.* Seismicity remotely triggered by the magnitude 7.3 Landers, California, earthquake. *Science* **250**, 1617–1623 (1993).
14. Brodsky, E., Karakostas, V. & Kanamori, H. A new observation of dynamically triggered regional seismicity: earthquakes in Greece following the August, 1999 Izmit, Turkey earthquake. *Geophys. Res. Lett.* **27**, 2742–2744 (2000).
15. Gombert, J., Bodin, P., Larson, K. & Dragert, H. Earthquake nucleation by transient deformations caused by the $M = 7.9$ Denali, Alaska, earthquake. *Nature* **427**, 621–624 (2004).
16. West, M., Sánchez, J. J. & McNutt, S. R. Periodically triggered seismicity at Mount Wrangell, Alaska, after the Sumatra earthquake. *Science* **308**, 1144–1146 (2005).
17. Miyazawa, M. & Mori, J. Detection of triggered deep low-frequency events from the 2003 Tokachi-oki earthquake. *Geophys. Res. Lett.* **32**, doi:10.1029/2005GL022539 (2005).
18. Suppe, J. Kinematics of arc-continent collision, flipping of subduction, and back-arc spreading near Taiwan. *Mem. Geol. Soc. China* **6**, 21–23 (1984).
19. Tsai, Y. B. Seismotectonics of Taiwan. *Tectonophysics* **125**, 17–38 (1986).
20. Ho, C. S. *An Introduction to the Geology of Taiwan: Explanatory Text of the Geologic Map of Taiwan* 2nd edn (Central Geological Survey, Taiwan, 1986).
21. Chi, W. R., Namson, J. & Suppe, J. Stratigraphic record of plate interactions in the Coastal Range of Eastern Taiwan. *Mem. Geol. Soc. China* **4**, 155–194 (1981).
22. Liu, C. C. & Yu, S. B. Vertical crustal movement in eastern Taiwan and its tectonic implications. *Tectonophysics* **183**, 111–119 (1990).
23. Hsieh, M. L., Liu, P. M. & Hsu, M. Y. Holocene tectonic uplift on the Hua-Tung coast, Eastern Taiwan. *Quaternary Int.* **115–116**, 47–70 (2004).
24. Yu, S. B. & Liu, C. C. Fault creep on the central segment of the Longitudinal Valley fault, Eastern Taiwan. *Proc. Geol. Soc. China* **32**, 209–231 (1989).
25. Lee, J. C., Angelier, J., Chu, H. T., Hu, J. C. & Jeng, F. S. Continuous monitoring of an active fault in a plate suture zone: a creepmeter study of the Chihshang Fault, eastern Taiwan. *Tectonophysics* **333**, 219–240 (2000).
26. Sacks, I. S., Suyehiro, S. & Evertson, D. W. Sacks–Evertson strainmeter, its installation in Japan and some preliminary results concerning strain steps. *Proc. Jpn Acad.* **47**, 707–712 (1971).
27. Kim, K. H. *et al.* Three-dimensional V_P and V_S structural models associated with the active subduction and collision tectonics in the Taiwan region. *Geophys. J. Int.* **162**, 204–220 (2005).
28. Okada, Y. Internal deformation due to shear and tensile faults in a half-space. *Bull. Seismol. Soc. Am.* **82**, 1018–1040 (1992).
29. Gao, S., Silver, P. G., Linde, A. T. & Sacks, I. S. Annual modulation of triggered seismicity following the 1992 Landers earthquake in California. *Nature* **406**, 500–504 (2000).
30. Shelly, D. R., Beroza, G. C., Ide, S. & Nakamura, S. Low-frequency earthquakes in Shikoku, Japan, and their relationship to episodic tremor and slip. *Nature* **442**, 188–191 (2006).

Supplementary Information is linked to the online version of the paper at www.nature.com/nature.

Acknowledgements We thank T. Lee for critically important work in initiating this project. M. Lee's expertise was valuable in site selection. J.-C. Rau and T.-S. Lee gave access to their property for borehole sites. H. M. Lee managed the archiving of data.

Author Information Reprints and permissions information is available at www.nature.com/reprints. Correspondence and requests for materials should be addressed to C.L. (liucc@sinica.edu.tw).

ERRATUM

doi:10.1038/nature08202

Slow earthquakes triggered by typhoons

ChiChing Liu, Alan T. Linde & I. Selwyn Sacks

Nature 459, 833–836 (2009)

In this Letter, address 1 was incorrectly listed. This oversight has now been rectified.